NJC

ROYAL SOCIETY OF CHEMISTRY

PAPER

View Article Online
View Journal | View Issue

Cite this: *New J. Chem.*, 2024, **48**, 2639

Synthesis of *N*-fused polycyclic indoles *via* a Pd-catalyzed multicomponent cascade reaction consisting of an amide-directed [3+1+1] annulation reaction of 3-diazo oxindole and isocyanides†

Pooja Soam,[a] Debasish Mandal [ab] and Vikas Tyagi *[ab]

Received 21st October 2023,
Accepted 4th January 2024

DOI: 10.1039/d3nj04886a

rsc.li/njc

Herein, we report a Pd-catalyzed multicomponent cascade reaction of 3-diazo oxindole and isocyanides to synthesize *N*-fused polycyclic indoles consisting of an *in situ* generated amide-assisted regioselective [3+1+1] annulation reaction. Additionally, a mechanism is proposed and investigated using DFT that strongly favors the role of amide in assisting the annulation reaction, which is further confirmed using control experiments.

Introduction

N-Fused polycyclic indoles have attracted great attention in synthetic chemistry due to their ubiquitous presence in several natural products and pharmaceutical agents (Fig. 1). They display a wide range of biological activities such as anticancer, anti-inflammatory, antimicrobial, antiatherogenic, antihypertensive, *etc.* Moreover, indole-fused heterocycles are imperative structural units of various agrochemicals, plastics, and dyes that are integrated into everyday life.[1a–g]

In this context, various combinations of polycyclic indole-fused heterocycles have been designed and synthesized in the past.[2a–e] However, the production of these moieties is very challenging due to the requirement of multistep synthesis, which is associated with their disadvantages. So, the development of novel and efficient methodologies to synthesize indole-fused heterocyclic scaffolds is highly admirable in synthetic chemistry. Throughout the significant progress made in this area, different methods have been developed to synthesize tricyclic oxazolo[3,2-*a*]indole moieties. In this context, Zhu *et al.* synthesized oxazolo[3,2-*a*]indolones *via* a visible light-induced aerobic dearomative reaction of *N*-substituted indoles in the presence of a Ru-catalyst (Scheme 1a).[3] Next, a metal- and solvent-free approach to synthesize oxazolo[3,2-*a*]indolones using propargylic alcohols and indole derivatives was developed by Oparina's group (Scheme 1b).[4] Recently, Wang and co-workers reported a cascade approach to synthesize oxazolo[3,2-*a*]indolones along with indolo [2,3-*b*] indoles in the presence of a rhodium catalyst at 130 °C (Scheme 1c).[5] However, most of these approaches are associated with certain limitations such as complex starting materials, longer reaction time, lower efficiency, and substrate scope.

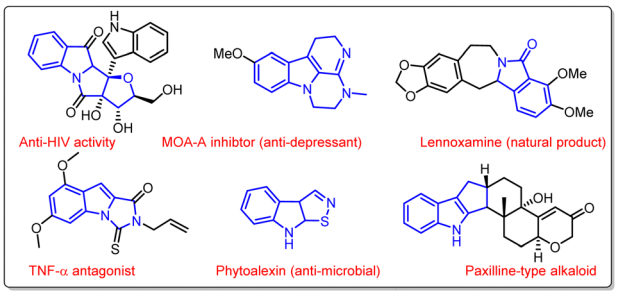

Fig. 1 Biologically important indole-fused heterocycles.

On the other hand, cascade or tandem reactions have been found to be very advantageous to improve synthetic efficiency in modern organic chemistry.[6a–e] Furthermore, the cascade reaction involves multiple bond-forming reactions in one pot, representing an attractive strategy towards the facile synthesis of novel molecular frameworks with less wastage of resources. In particular, transition metal-catalyzed one-pot cascade reactions are being used to generate novel fused heterocycles.[7a–c]

[a] *School of Chemistry and Biochemistry, Thapar Institute of Engineering and Technology, Patiala-147004, Punjab, India. E-mail: vikas.tyagi@thapar.edu*
[b] *Centre of Excellence for Emerging Materials, Thapar Institute of Engineering and Technology, Patiala-147004, Punjab, India*

† Electronic supplementary information (ESI) available: X-ray crystal data of compound **3a**, copies of ^{1}H NMR and ^{13}C NMR data of the compounds (**3a–3q**, **4**), computational details, optimized transition states and optimized Cartesian coordinates and electronic energies. CCDC 2291510. For ESI and crystallographic data in CIF or other electronic format see DOI: **https://doi.org/10.1039/d3nj04886a**

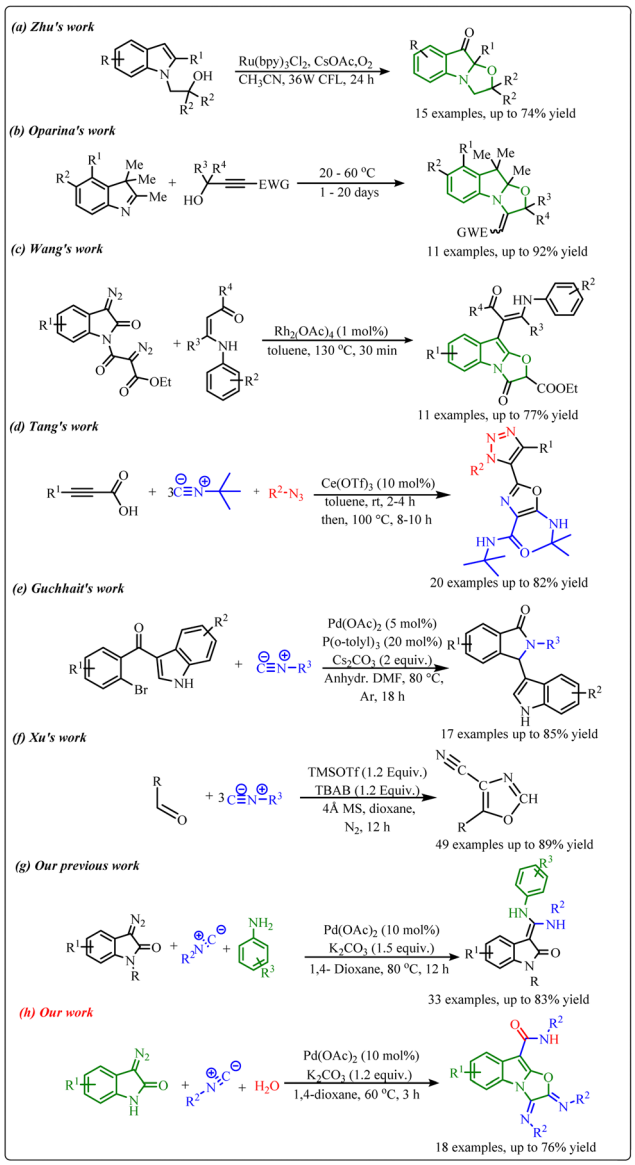

Scheme 1 (a)–(c) Recent approaches to synthesizing tricyclic oxazolo-[3,2-*a*]indole derivatives, (d)–(f) recent isocyanide insertion approaches, (g) our previous work, and (h) recent work.

Interestingly, isocyanides have been considered important substrates for transition metal-catalyzed one-pot cascade reactions since they can react both as a nucleophile or an electrophile in chemical reactions.[8a–e] In this context, several cascade reactions using isocyanides have been developed in the past. Recently, Tang's group reported a cerium triflate catalyzed triple isocyanide insertion approach to develop a library of oxazole derivatives.[9] Next, Guchhait *et al.* developed a cascade C–H activation methodology to construct bicyclic indolyl motifs *via* intramolecular isocyanide insertion using Pd-catalysts.[10] Another efficient approach towards consecutive triple isocyanide insertion into aldehydes to synthesize a broad library of 4-cyano oxazole derivatives was reported by Xu and co-workers. (Scheme 1d–f)[11] Also, we have developed a Pd-catalysed one-pot cascade reaction to access benzoxazine-fused 1,2,3-triazoles

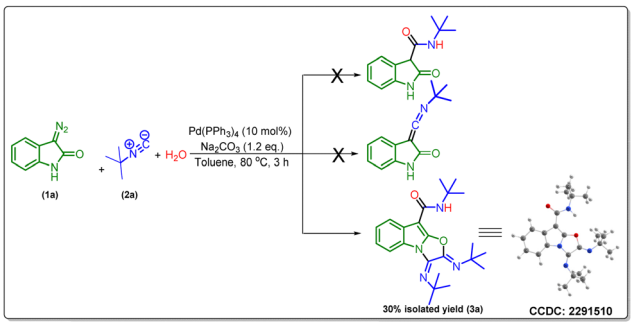

Scheme 2 Possible structures under a Pd-catalyzed reaction.

using *N*-aryl-α-(tosylhydrazone)acetamides with isocyanide.[12] In continuation of our efforts to develop novel cascade reactions by the use of isocyanide and diazo compounds (Scheme 1g),[13] herein, we have developed a Pd-catalysed multicomponent cascade reaction of 3-diazo oxindole, isocyanide, and H_2O to generate tricyclic oxazolo[3,2-*a*]indole scaffolds (Scheme 1h).

Results and discussion

Initially, we envisioned the synthesis of indole-3-acetamide *via* the formation of indole-based ketenimine intermediates by the reaction of isocyanide and 3-diazo oxindole as previously reported by our group and others. To actualize our hypothesis, we set up a reaction of *tert*-butyl isocyanide, water, and 3-diazo oxindole using 10 mol% of $Pd(PPh_3)_4$ and 1.2 equivalent of

Table 1 Optimization of the reaction conditions[a]

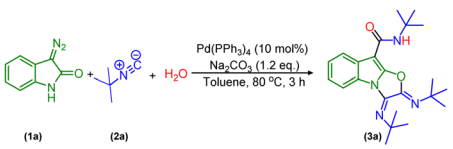

Entry	Deviation from standard conditions	Yield[b] (%)
1	No deviation	30
2	$Cu(OAc)_2$ instead of $Pd(PPh_3)_4$	—
3	$Rh_2(OAc)_4$ instead of $Pd(PPh_3)_4$	—
4	$Pd(OAc)_2$ instead of $Pd(PPh_3)_4$	56
5	$Pd(TFA)_2$ instead of $Pd(PPh_3)_4$	38
6	$Pd(OPiv)_2$ instead of $Pd(PPh_3)_4$	31
7	No catalyst	—
8	Cs_2CO_3 instead of Na_2CO_3	51
9	K_2CO_3 instead of Na_2CO_3	59
10	KO*t*-Bu instead of Na_2CO_3	35
11	NEt_3 instead of Na_2CO_3	43
12	DBU instead of Na_2CO_3	39
13	1,4-Dioxane instead of toluene	64
14	60 °C	71
15	50 °C	36
16	40 °C	Trace
17	rt	—
18	2 equiv. of H_2O	60
19	No H_2O	20

[a] Reaction conditions: 3-diazo oxindole **1a** (1.0 equiv., 0.31 mmol, and 50 mg), *tert*-butyl isocyanide **2a** (3.2 equiv., 113 μL, and 0.99 mmol), H_2O (1.0 equiv., 5.6 μL), Pd-catalyst (10 mol%), base (1.2 equiv.), and solvent (2 ml), for 3 h. [b] Isolated yield.

Na_2CO_3 in toluene as a solvent at 80 °C, and obtained the product in a 30% isolated yield. However, characterization techniques such as ^{1}H-NMR, ^{13}C-NMR, HRMS, and X-ray confirm the unprecedented formation of a tricyclic oxazolo[3,2-*a*]-indole derivative (Scheme 2).

Drawing encouragement from these findings, next, we decided to optimize the reaction conditions to improve the yield of the multicomponent cascade reaction by selecting 3-diazo oxindole (**1a**), *tert*-butyl isocyanide (**2a**), and H_2O as model substrates. Initially, we screened different transition metal catalysts such as $Cu(OAc)_2$ and $Rh_2(OAc)_4$ in addition to $Pd(PPh_3)_4$, and unexpectedly the reaction worked only with the Pd-catalyst (Table 1, entries 1–3). Afterward, we examined different palladium-based catalysts like $Pd(OAc)_2$, $Pd(TFA)_2$, $Pd(OPiv)_2$, $PdCl_2$, $PdCl_2(NCC_6H_5)_2$, $Pd(DPPF)Cl_2$, $Pd_2(dba)_3$ *etc.* and obtained product (**3a**) in a maximum yield, *i.e.* 56% when 10 mol% of $Pd(OAc)_2$ was added as a catalyst (Table 1, entry 4–6) and (Table S2, entries 1–4, ESI†). However, on decreasing the amount of $Pd(OAc)_2$ from 10 mol% to 5 mol%, the yield of the model reaction got decreased (Table S2, entry 5, ESI†). Also, it must be noticed that the reaction did not work in the absence of a palladium catalyst (Table 1, entry 7). Next, we screened different bases and found that the reaction provided a maximum yield in the case of K_2CO_3 as compared to other bases such as Na_2CO_3, Cs_2CO_3, KO*t*-Bu, NEt_3 and DBU (Table 1, entries 8–12). Also, it was observed that in the absence of a base, the yield of product (**3a**) decreased, up to a 27% yield (Table S2, entry 6, ESI†). Furthermore, toluene was replaced by various solvents like 1,4-dioxane, CH_3CN, DMF, DMSO, and THF; however, 1,4-dioxane was found to be the best solvent (Table 1, entry 13) and (Table S2, entries 7–10, ESI†). Besides, there was no improvement in the outcome of the model reaction observed while adding different additives like AgOAc and CsOAc (Table S2, entries 11 and 12, ESI†). Moreover, temperature variation significantly affected the outcome of the model reaction. In particular, decreasing the temperature from 80 °C to 60 °C increases the yield of **3a** to 71% (Table 1, entry 14). Then, the yield of **3a** was reduced by further decreasing the temperature to 50 °C (Table 1, entry 15). The reaction was almost diminished below 50 °C and the product was

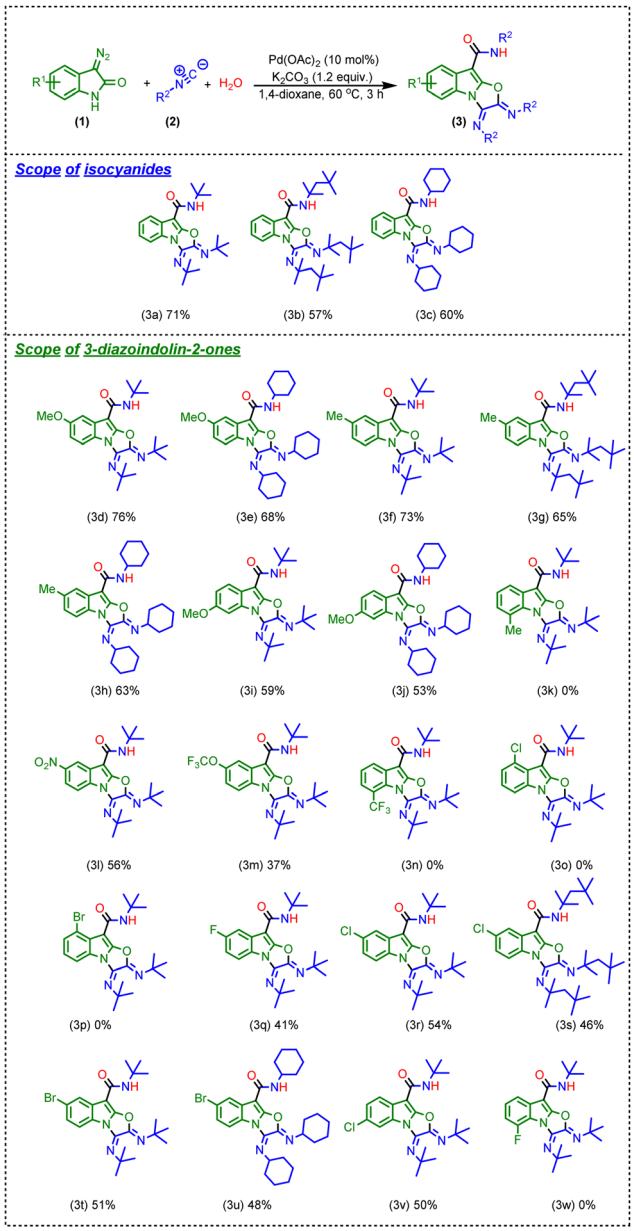

Scheme 3 The substrate scope of the Pd-catalyzed multicomponent cascade reaction. Reaction conditions: 3-diazo oxindoles (1) (1.0 equiv.), isocyanides (2) (3.2 equiv.), H_2O (3) (1.0 equiv.), $Pd(OAc)_2$ (10 mol%), K_2CO_3 (1.2 equiv.), and 1,4-dioxane (2 mL), for 3 h, at 60 °C.

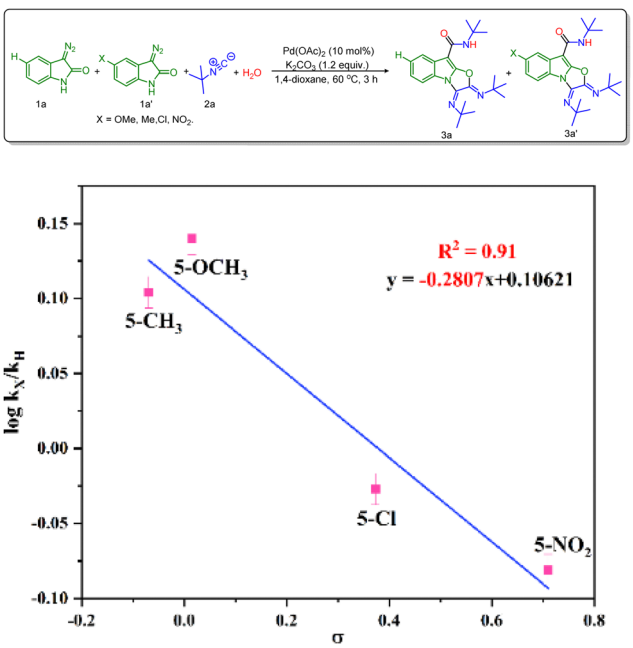

Scheme 4 Hammett plot for the reaction of isocyanide with electronically varied 3-diazo oxindoles.[a] [a]Reaction conditions: 3-diazo oxindole **1a** (1.0 equiv., 0.31 mmol), substituted 3-diazo oxindole **1a**′ (1.0 equiv., 0.31 mmol), *tert*-butyl isocyanide **2a** (3.2 equiv., 0.99 mmol), H_2O (1.0 equiv.), $Pd(OAc)_2$ (10 mol%), K_2CO_3 (1.2 equiv.), and 1,4-dioxane (2 mL), for 3 h, at 60 °C.

observed only in trace amounts at 40 °C (Table 1, entries 16 and 17). Subsequently, increasing the equivalent of water slightly decreased the yield to 60% (Table 1, entry 18). Noticeably, in the absence of water, only a 20% yield of product **3a** was observed, which suggests the requirement of water in an equimolar amount in this transformation (Table 1, entry 19). Also, the molar ratio of the substrates was varied; however, 1 : 3.2 : 1 of 3-diazo oxindole, *tert*-butyl isocyanide, and water, respectively, remained the best ratio (Table S2, entries 13–16, ESI†).

After having the optimized reaction conditions in hand, we evaluated the feasibility of the reaction with different isocyanides as well as 3-diazo oxindole as revealed in Scheme 3.

Firstly, we have replaced *tert*-butyl isocyanide with 1,1,3,3-tetramethyl butyl isocyanide or cyclohexyl isocyanide, and as a result, the corresponding products (**3b** and **3c**) were obtained in slightly lower yields in comparison of the product **3a** (Scheme 3). These results represent the structural role of isocyanides; as the steric hindrance increases, the yield of the reaction decreases. Besides, we have tried reactions with other isocyanides like *p*-methoxy phenyl isocyanide and *p*-toluene sulphonyl methyl-isocyanide; however, no product formation was observed with these isocyanides. Next, we have examined the effect of various electron-donating, electron-withdrawing, and halide substituents at different positions of 3-diazo oxindole. Initially, a range of electron-donating groups at different positions of the phenyl ring of 3-diazo oxindole were tested. Noticeably, in the case of 5-OMe-substituted 3-diazo oxindole, the reaction provided products (**3d**) and (**3e**) in 76% and 68% yields, respectively, whereas the reaction provided moderate to good yields of the desired products when 5-CH_3-substituted 3-diazo oxindole was employed with *tert*-butyl isocyanide, 1,1,3,3-tetramethyl butyl isocyanide, and cyclohexyl isocyanide, respectively (**3f–h**, Scheme 3). Also, 6-OMe-substituted 3-diazo oxindole provided products **3i** and **3j** in slightly lower yields, *i.e.*, 59 and 53% (Scheme 3). It should be noted that the yield diminished when the electron-donating group, *i.e.* –CH_3, was incorporated at the 7-position of 3-diazo oxindole and it might be due to hindrance enhancement near the fringe where the reaction occurred (**3k**, Scheme 3). This abatement of yield indicated the significance of the electronic and steric effects of the substituents at different positions of 3-diazo oxindole. Next, electron-withdrawing groups *i.e.*, 5-nitro and 5-OCF_3 substituted 3-diazo oxindole were used in the reaction and the products (**3l** and **3m**) were attained in 56% and 37% isolated yield (Scheme 3), which slightly lower in comparison to 3-diazo oxindole having an electron-donating group at the same position. However, there was no product formation observed when 7-CF_3-containing 3-diazo oxindole was employed in the reaction (**3n**, Scheme 3). Afterward, we examined the effect of halides at different positions of 3-diazo oxindoles and found that in the case of 4-Cl and 4-Br substitutions, the yields almost diminished (**3o** and **3p**, Scheme 3). Next, 5-F-substituted 3-diazo oxindole provides product **3q** in a lower yield as compared to 3-diazo oxindole having electron-withdrawing and -donating groups. Next, 5-Cl- and 5-Br-substituted 3-diazo oxindoles were employed in the reaction, and the corresponding products (**3r** to **3u**) were obtained in lower yields, *i.e.*, 46 to 54% as compared to electron-donating

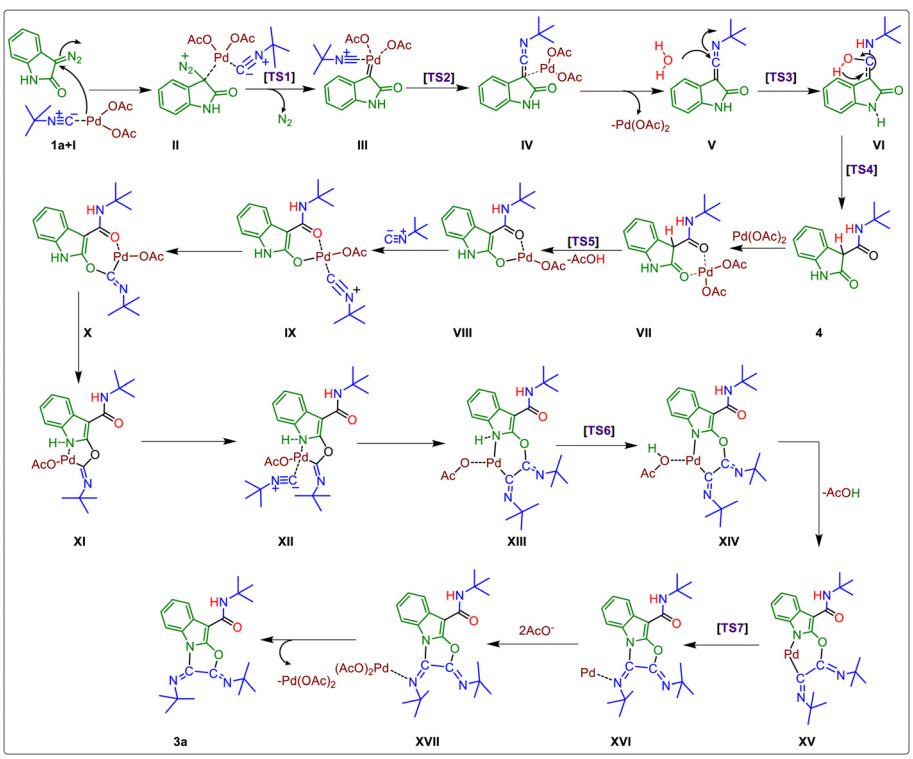

Fig. 2 The plausible mechanism for Pd-catalyzed multicomponent cascade reaction.

and electron-withdrawing substitutions at 3-diazo oxindole. However, the reaction provided the product in a moderate yield when 6-Cl-substituted 3-diazo oxindole was used in the reaction (**3v**, Scheme 3). Again, halide substitution at the 7-position of 3-diazo oxindole did not work (**3w**, Scheme 3).

Besides, a Hammet study was performed to get further information about the effect of substituents on the rate of the reaction.[14] In this view, 3-diazo oxindole having substituents like 5-OMe, 5-Me, 5-Cl and 5-NO_2 along with unsubstituted 3-diazo oxindole was employed in the multicomponent reaction (Scheme 4). The best linear fit ($R^2 = 0.91$) was achieved using the standard σ_p parameters *vs.* $\log k_X/k_H$, providing a ρ value (slope value) of −0.28. The value of ρ is less than 1, which indicates that a positive charge is built up during the rate-determining step. Also, the positive slope value suggests that the rate of reaction increases in the presence of the electron-donating groups.

Next, we have presented a plausible mechanism for the synthesis of tricyclic oxazolo[3,2-*a*]indole scaffolds as shown in Fig. 2.[15] Initially, *tert*-butyl isocyanide reacts with $Pd(OAc)_2$ to generate complex (**I**).[12,16a–d] Then, *tert*-butyl isocyanide acts as a neutral ligand in complex (**I**), and palladium remains in its divalent oxidation state. Complex (**I**) then linked with the 3-diazo oxindole (**1a**) substrate to generate square planar complex (**II**) that served as our starting complex. In this context, Fig. 2 shows the overall mechanism's steps, and Fig. 3(a) displays the associated DFT-computed potential free energy profiles in relation to the energies of the initial complex (I + **1a**). Furthermore, Fig. 3(b) depicts the optimized transition states computed at the B3LYP/6-31+G(d,p) level of theory.

Furthermore, the elimination of N_2 from complex (**II**) took place and generated Pd–carbene complex (**III**) *via* **TS1** (Fig. 3(b)) with the free energy of activation $\Delta G^{\ddagger}$ = 29.2 kcal mol^{-1}. The next step is the migration of isocyanide into the Pd–carbene complex through the three-membered ring transition state, **TS2** (Fig. 3(b)), which has a 21.5 kcal mol^{-1} free energy of activation and produces Pd-ketenimine complex (**IV**), which readily releases $Pd(OAc)_2$ to form highly unstable ketenimine intermediate (**V**). Furthermore, H_2O is connected to the central electrophilic carbon of the ketenimine intermediate (**V**) with simultaneous proton transfer to the nitrogen of the isocyanide unit *via* **TS3** (Fig. 3(b)) with $\Delta G^{\ddagger}$ = 13.3 kcal mol^{-1} to form intermediate **VI**, which is stabilized by −37.2 kcal mol^{-1} from **TS3** (Fig. 3(b)).

After that, the tautomerization step takes place *via* proton transfer to the C-3 carbon of **VI** from the OH group to form amide intermediate (*N*-(*tert*-butyl)-2-oxoindoline-3-carboxamide) **4**, through **TS4** (Fig. 3(b)) with a barrier of 40.3 kcal mol^{-1}.[17a,b] Afterward, *N*-(*tert*-butyl)-2-oxoindoline-3-carboxamide (**4**) interacts with palladium acetate to form six-membered complex **VII**,

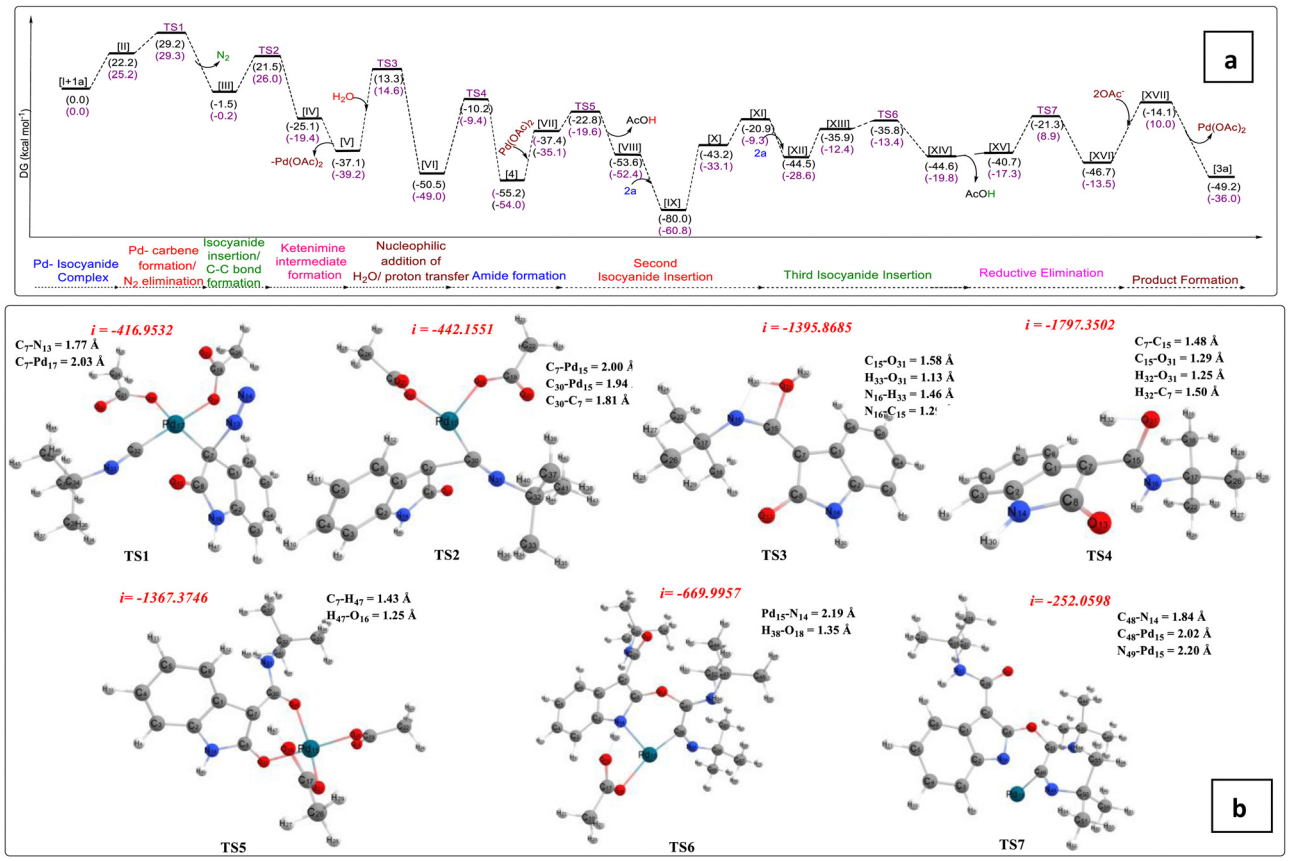

Fig. 3 (a) The potential energy profiles computed at the M06/6-31++G(2d,2p)/B3LYP/6-31+G(d,p) level of theory related to the plausible mechanism represented in Fig. 2. (b) Optimized transition states computed at the B3LYP/6-31+G(d,p) level of theory.

which releases the proton from the C-3 position and acetate group from the palladium catalyst as acetic acid to form complex **VIII** *via* transition state **TS5** (Fig. 3(b)) with $\Delta G^{\ddagger}$ = 14.6 kcal mol^{-1}. During this step, the oxidation state of Pd remains unchanged, which is further coordinated with a second *tert*-butyl isocyanide to form a highly stabilized (–80.0 kcal mol^{-1}) tetravalent Pd-containing intermediate **IX**. Then, the amidic C=O group at the C2-position gets activated and an isocyanide unit is inserted into the Pd–O bond to form seven-membered complex **X**, which readily converts to five-membered palladacyclic intermediate complex **XI** having an energy of 22.3 kcal mol^{-1}, higher than complex **X**. Next, the third *tert*-butyl isocyanide proceeds to link to the Pd atom of complex (**XI**) to form stable tetravalent complex **XII**. Again, this isocyanide is inserted into the Pd–C bond and regains its six-membered intermediate to form intermediate **XIII**, having a higher energy of 8.6 kcal mol^{-1} from complex **XII**. The acetate group present at the palladacyclic intermediate (**XIII**) abstracts the N–H proton *via* transition state **TS6** (Fig. 3(b)), which is located at the point of –35.8 kcal mol^{-1} in the PES and form another complex **XIV**, which possesses 44.6 kcal mol^{-1} less energy from the starting complex. Afterward, complex **XIV** releases AcOH and forms another complex **XV** having slightly higher energy (3.8 kcal mol^{-1}) than complex **XIII**. Finally, C–N bond formation takes place *via* transition state, **TS7** (Fig. 3(b)), having $\Delta G^{\ddagger}$ = 19.4 kcal mol^{-1} from complex **XV** and forms complex **XVI**. Afterward, reductive elimination of palladium occurs in the form of palladium acetate to give the final product (**3a**) through intermediate **XVII**.

Finally, several control studies were carried out to confirm the role of amide in this synthesis. We set up a reaction using *tert*-butyl 3-diazo-2-oxoindoline-1-carboxylate (**1p**) with *tert*-butyl isocyanide under standard reaction conditions (Scheme 5i) and got product *N*-(*tert*-butyl)-2-oxoindoline-3-carboxamide (**4**) in a 78% yield. In continuation, we performed a reaction of *N*-(*tert*-butyl)-2-oxoindoline-3-carboxamide (**4**) with *tert*-butyl isocyanide under the same reaction conditions. Delightfully, we got the desired product (**3a**) in a good yield (Scheme 5ii), which confirmed the formation of *N*-(*tert*-butyl)-2-oxoindoline-3-carboxamide (**4**) as an intermediate in this transformation. To further confirm the role of *in situ* generated amide, we have tried the reaction with three different oxindole derivatives such as ethyl 2-oxoindoline-3-carboxylate (**5**), indolin-2-one (**6**), and 3-hydroxy-3-(2-oxopropyl)indolin-2-one (**7**). Surprisingly there was no reaction with these substrates {Scheme 5(iii–v)}. So, these control experiments suggest that the amide group at the C-3 position of oxindole is required to assist the reaction for further steps.[8,18] Next, we tried a reaction with D_2O in place of H_2O, and product formation was confirmed with HRMS analysis. HRMS data of the crude reaction mixture showed a peak at 398.2648, equivalent to a deuterated amide-based product. Hence, this experiment suggests the participation of H_2O molecules in the formation of amide {Scheme 5(vi)}.

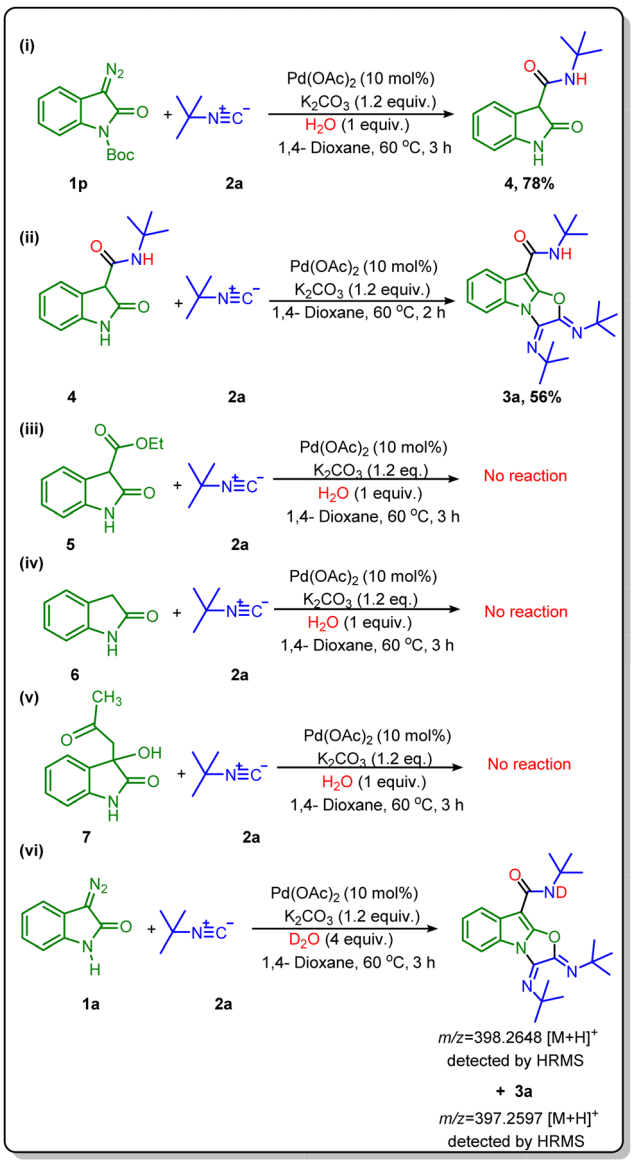

Scheme 5 Control experiments. Reaction conditions for (i)–(v): substrates 1p/4/5/6 or 7 (1 equiv.), isocyanides (2) (3.2 equiv.), H_2O (1.0 equiv.), $Pd(OAc)_2$ (10 mol%), K_2CO_3 (1.2 equiv.), and 1,4-dioxane (2 mL), for 3 h, at 60 °C. (vi) **1a** (1 equiv.), isocyanides (2) (3.2 equiv.), D_2O (4.0 equiv.), $Pd(OAc)_2$ (10 mol%), K_2CO_3 (1.2 equiv.), and 1,4-dioxane (2 mL), for 3 h, at 60 °C.

Conclusions

In summary, we have developed a Pd-catalysed and amide-assisted multicomponent reaction of 3-diazo oxindole, isocyanide, and water to generate oxazole-fused indole scaffolds. The functional group tolerance at different positions of 3-diazo oxindole along with different isocyanides was tested and the corresponding products were obtained in 37–76% isolated yields. Besides, a DFT study was performed to get an overview of the proposed mechanism, which recommended that the reaction involved amide formation at the C-3 position *via* isocyanide insertion, which subsequently assisted a [3+1+1] annulation reaction to furnish oxazole-fused indoles. Also, the role of *in situ*-generated amide to assist the annulation

reaction was confirmed by setting up different control experiments.

Procedure and characterization

General procedure to synthesize (2*Z*,3*E*)-*N*-(*tert*-butyl)-2,3-bis(*tert*-butylimino)-2,3-dihydrooxazolo[3,2-*a*]indole-9-carboxamide (3a–3q)

In a glass tube equipped with a stirrer bar, 3-diazo oxindole (1.0 equiv., 50 mg, 0.31 mmol), H_2O (1.0 equiv., 5.6 μL, 0.31 mmol), $Pd(OAc)_2$ (10 mol%, 7 mg), K_2CO_3 (1.5 equiv., 65 mg, 0.47 mmol) and 2 mL of 1,4-dioxane as a solvent were added. Then, the resulting reaction mixture was stirred at 60 °C in a preheated oil bath and *tert*-butyl isocyanide (3.2 equiv., 116 μL, 0.99 mmol) was added slowly with the help of a syringe. After completion of the reaction as indicated by TLC, work-up of the reaction mixture was done using ethyl acetate and distilled water in a 2 : 1 ratio followed by evaporation of volatiles under a reduced pressure. Next, the crude mixture was purified by column chromatography using ethyl acetate in hexane as an eluent affording the corresponding (2*Z*,3*E*)-*N*-(*tert*-butyl)-2,3-bis(*tert*-butylimino)-2,3-dihydrooxazolo[3,2-*a*]indole-9 carboxamide (**3a–3w**) in 37–76% yields.

Characterization data

^{1}H NMR (400 MHz, $CDCl_3$) and $^{13}C\{^1H\}$ NMR (100 MHz, $CDCl_3$) spectra of (2*Z*,3*E*)-*N*-(*tert*-butyl)-2,3-bis(*tert*-butylimino)-2,3-dihydrooxazolo[3,2-*a*]indole-9-carboxamide (3a). Purification by column chromatography (EtOAc : hexane v/v 1 : 19) afforded **3a**; yellow solid, yield = 71% (88 mg, 0.223 mmol), ^{1}H NMR (400 MHz, $CDCl_3$): 8.20 (d, J = 7.2 Hz, 1H), 7.89 (d, J = 7.6 Hz, 1H), 7.27–7.18 (m, 2H), 5.70 (s, 1H), 1.52 (s, 9H), 1.50 (s, 9H), 1.47 (s, 9H) ppm. $^{13}C\{^1H\}$ NMR (100 MHz, $CDCl_3$): δ 162.3, 148.8, 136.5, 133.0, 128.9, 127.4, 124.2, 123.1, 121.9, 112.6, 87.8, 57.6, 55.9, 51.4, 30.0, 29.5, 29.4 ppm. HRMS (ESI-TOF) m/z: $[M + H]^+$ calcd for $C_{23}H_{33}N_4O_2$ 397.2604; found 397.2601.

^{1}H NMR (400 MHz, $CDCl_3$) and $^{13}C\{^1H\}$ NMR (100 MHz, $CDCl_3$) spectra of (2*Z*,3*E*)-*N*-(2,4,4-trimethylpentan-2-yl)-2,3-bis((2,4,4-trimethylpentan-2-yl)imino)-2,3-dihydrooxazolo[3,2-*a*]-indole-9-carboxamide (3b). Purification by column chromatography (EtOAc : hexane v/v 1 : 19) afforded **3b**: yellow solid, yield = 57% (101 mg, 0.179 mmol), ^{1}H NMR (400 MHz, $CDCl_3$): 8.24 (d, J = 8 Hz, 1H), 7.94 (d, J = 8 Hz, 1H), 7.28–7.19 (m, 2H), 5.62 (s, 1H), 2.01 (s, 2H), 1.92 (s, 4H), 1.58 (s, 6H), 1.55 (s, 6H), 1.51 (s, 6H), 1.03 (s, 9H), 1.00 (s, 9H), 1.00 (s, 9H) ppm. $^{13}C\{^1H\}$ NMR (100 MHz, $CDCl_3$): δ 162.3, 148.4, 136.2, 131.8, 129.0, 127.5, 124.2, 123.1, 122.1, 112.5, 87.7, 61.4, 60.0, 55.3, 54.3, 54.1, 51.1, 32.2, 32.1, 32.0, 31.9, 31.7, 31.6, 31.0, 30.3, 30.2 ppm. HRMS (ESI-TOF) m/z: $[M + H]^+$ calcd for $C_{35}H_{57}N_4O_2$ 565.4487; found 565.4487.

^{1}H NMR (400 MHz, $CDCl_3$) and $^{13}C\{^1H\}$ NMR (100 MHz, $CDCl_3$) spectra of (2*Z*,3*E*)-*N*-cyclohexyl-2,3-bis(cyclohexylimino)-2,3-dihydrooxazolo[3,2-*a*]indole-9-carboxamide (3c). Purification by column chromatography (EtOAc : hexane v/v 1 : 19) afforded **3c**: yellow solid, yield = 60% (89 mg, 0.188 mmol), ^{1}H NMR (400 MHz, $CDCl_3$): 8.11 (d, J = 8.0 Hz, 1H), 7.87 (d, J = 8.0 Hz, 1H), 7.27–7.19 (m, 2H), 5.78 (d, J = 8.0 Hz, 1H), 4.78–4.71 (m, 1H), 4.09–3.97 (m, 2H), 2.00–1.26 (m, 30H) ppm. $^{13}C\{^1H\}$ NMR (100 MHz, $CDCl_3$): δ 160.7, 148.1, 138.2, 133.3, 127.6, 126.1, 123.1, 122.1, 120.5, 111.6, 86.7, 56.3, 55.3, 46.2, 32.9, 32.1, 32.0, 24.8, 24.7, 24.6, 23.4, 23.3, 22.7 ppm. HRMS (ESI-TOF) m/z: $[M + H]^+$ calcd for $C_{29}H_{39}N_4O_2$ 475.3069; found 475.3073.

^{1}H NMR (400 MHz, $CDCl_3$) and $^{13}C\{^1H\}$ NMR (100 MHz, $CDCl_3$) spectra of (2*Z*,3*E*)-*N*-(*tert*-butyl)-2,3-bis(*tert*-butylimino)-7-methoxy-2,3-dihydrooxazolo[3,2-*a*]indole-9-carboxamide (3d). Purification by column chromatography (EtOAc : hexane v/v 1 : 19) afforded **3d**: yellow solid, yield = 76% (86 mg, 0.201 mmol), ^{1}H NMR (400 MHz, $CDCl_3$): δ 7.77 (d, J = 2.4 Hz, 1H), 7.74 (s, 1H), 6.80 (dd, J = 8.8, 2.8 Hz, 1H), 5.70 (s, 1H), 3.86 (s, 3H), 1.50 (s, 9H), 1.49 (s, 9H), 1.46 (s, 9H) ppm. $^{13}C\{^1H\}$ NMR (100 MHz, $CDCl_3$): δ 162.6, 157.1, 149.2, 136.4, 132.8, 130.0, 121.8, 113.3, 112.2, 104.5, 87.8, 57.6, 55.8, 51.4, 30.0, 29.5, 29.4 ppm. HRMS (ESI-TOF) m/z: $[M + H]^+$ calcd for $C_{24}H_{35}N_4O_3$ 427.2709; found 427.2712.

^{1}H NMR (400 MHz, $CDCl_3$) and $^{13}C\{^1H\}$ NMR (100 MHz, $CDCl_3$) spectra of (2*Z*,3*E*)-*N*-cyclohexyl-2,3-bis(cyclohexylimino)-7-methoxy-2,3-dihydrooxazolo[3,2-*a*]indole-9-carboxamide (3e). Purification by column chromatography (EtOAc : hexane v/v 1 : 19) afforded **3e**: yellow solid, yield = 68% (137 mg, 0.272 mmol), ^{1}H NMR (400 MHz, $CDCl_3$): 7.75–7.73 (m, 2H), 6.81 (dd, J = 8.4, 2.4 Hz, 1H), 5.74 (d, J = 8.0 Hz, 1H), 4.76–4.69 (m, 1H), 3.86 (s, 3H), 2.00–1.27 (m, 30H) ppm. $^{13}C\{^1H\}$ NMR (100 MHz, $CDCl_3$): δ 162.0, 157.1, 149.4, 139.2, 134.3, 130.0, 121.7, 113.5, 112.1, 104.7, 87.7, 57.4, 56.4, 55.7, 47.3, 34.0, 33.2, 33.1, 29.8, 25.85, 25.77, 25.72, 24.5, 24.4, 23.8 ppm. HRMS (ESI-TOF) m/z: $[M + H]^+$ calcd for $C_{30}H_{41}N_4O_3$ 505.3179; found 505.3179.

^{1}H NMR (400 MHz, $CDCl_3$) and $^{13}C\{^1H\}$ NMR (100 MHz, $CDCl_3$) spectra of (2*Z*,3*E*)-*N*-(*tert*-butyl)-2,3-bis(*tert*-butylimino)-7-methyl-2,3-dihydrooxazolo[3,2-*a*]indole-9-carboxamide (3f). Purification by column chromatography (EtOAc : hexane v/v 1 : 19) afforded **3f**: yellow solid, yield = 73% (86.5 mg, 0.211 mmol), ^{1}H NMR (400 MHz, $CDCl_3$): 8.04 (s, 1H), 7.75 (d, J = 8.0 Hz, 1H), 7.01 (dd, J = 1.2, 8.4 Hz, 1H), 5.69 (s, 1H), 2.41 (s, 3H), 1.51 (s, 9H), 1.49 (s, 9H), 1.46 (s, 9H) ppm. $^{13}C\{^1H\}$ NMR (100 MHz, $CDCl_3$): δ 162.6, 148.9, 136.6, 133.9, 132.9, 129.0, 125.6, 124.2, 122.1, 112.2, 87.6, 57.6, 55.8, 51.4, 30.0, 29.5, 29.3, 21.8 ppm. HRMS (ESI-TOF) m/z: $[M + H]^+$ calcd for $C_{24}H_{35}N_4O_2$ 411.2760; found 411.2755.

^{1}H NMR (400 MHz, $CDCl_3$) and $^{13}C\{^1H\}$ NMR (100 MHz, $CDCl_3$) spectra of (2*Z*,3*E*)-7-methyl-*N*-(2,4,4-trimethylpentan-2-yl)-2,3-bis((2,4,4-trimethylpentan-2-yl)imino)-2,3-dihydrooxazolo-[3,2-*a*]indole-9-carboxamide (3g). Purification by column chromatography (EtOAc : hexane v/v 1 : 19) afforded **3g**: yellow solid, yield = 65% (108 mg, 0.188 mmol), ^{1}H NMR (400 MHz, $CDCl_3$): 8.08 (s, 1H), 7.80 (d, J = 8.0 Hz, 1H), 7.02 (dd, J = 8.0 Hz, 1.2 Hz, 1H), 5.61 (s, 1H), 2.42 (s, 3H), 2.00 (s, 2H), 1.92 (s, 2H), 1.91 (s, 2H), 1.57 (s, 6H), 1.54 (s, 6H), 1.51 (s, 6H), 1.02 (s, 9H), 1.00 (s, 9H), 0.99 (s, 9H) ppm. $^{13}C\{^1H\}$ NMR (100 MHz, $CDCl_3$): δ 162.5, 148.6, 136.3, 133.9, 131.7, 129.2, 125.6, 124.2, 122.2, 112.1, 87.4, 61.4, 59.9, 55.3, 54.4, 54.1, 51.0, 32.2, 32.1, 32.0, 31.9, 31.7, 31.6,

31.0, 30.3, 30.1, 29.8, 21.8 ppm. HRMS (ESI-TOF) *m*/*z*: $[M + H]^+$ calcd for $C_{36}H_{59}N_4O_2$ 579.4638; found 579.4632.

^{1}H NMR (400 MHz, $CDCl_3$) and $^{13}C\{^1H\}$ NMR (100 MHz, $CDCl_3$) spectra of (2*Z*,3*E*)-*N*-cyclohexyl-2,3-bis(cyclohexylimino)-7-methyl-2,3-dihydrooxazolo[3,2-*a*]indole-9-carboxamide (3h). Purification by column chromatography (EtOAc : hexane v/v 1 : 19) afforded **3h**: yellow solid, yield = 63% (88.8 mg, 0.182 mmol), ^{1}H NMR (400 MHz, $CDCl_3$): 7.95 (s, 1H), 7.73 (d, 1H), 7.03 (dd, J = 8.4, 1.2 Hz, 1H), 5.75 (d, J = 7.6 Hz, 1H), 4.77–4.71 (m, 1H), 4.08–3.96 (m, 2H), 2.43 (s, 3H), 1.82–1.24 (m, 30H) ppm. $^{13}C\{^1H\}$ NMR (100 MHz, $CDCl_3$): δ 160.8, 148.1, 138.3, 133.3, 132.8, 127.8, 124.3, 123.2, 120.8, 111.3, 86.4, 56.3, 55.3, 46.2, 32.9, 32.1, 32.0, 28.6, 24.74, 24.67, 24.6, 23.4, 23.3, 22.7, 20.8 ppm. HRMS (ESI-TOF) *m*/*z*: $[M + H]^+$ calcd for $C_{30}H_{41}N_4O_2$ 489.3230; found 489.3224.

^{1}H NMR (400 MHz, $CDCl_3$) and $^{13}C\{^1H\}$ NMR (100 MHz, $CDCl_3$) spectra of (2*Z*,3*E*)-*N*-(*tert*-butyl)-2,3-bis(*tert*-butylimino)-6-methoxy-2,3-dihydrooxazolo[3,2-*a*]indole-9-carboxamide (3i). Purification by column chromatography (EtOAc : hexane v/v 1 : 19) afforded **3i**: yellow solid, yield = 59% (66.5 mg, 0.156 mmol), ^{1}H NMR (400 MHz, $CDCl_3$): δ 8.06 (d, J = 8.8 Hz, 1H), 7.49 (d, J = 2.4 Hz, 1H), 6.86 (dd, J = 8.8 Hz, 2.4 Hz, 1H), 5.67 (s, 1H), 3.83 (s, 3H), 1.51 (s, 9H), 1.49 (s, 9H), 1.46 (s, 9H) ppm. $^{13}C\{^1H\}$ NMR (100 MHz, $CDCl_3$): δ 162.4, 156.7, 147.9, 136.8, 133.1, 128.1, 122.5, 122.4, 111.6, 98.2, 87.7, 57.5, 55.9, 55.7, 51.3, 30.0, 29.5, 29.4 ppm. HRMS (ESI-TOF) *m*/*z*: $[M + H]^+$ calcd for $C_{24}H_{35}N_4O_3$ 427.2709; found 427.2714.

^{1}H NMR (400 MHz, $CDCl_3$) and $^{13}C\{^1H\}$ NMR (100 MHz, $CDCl_3$) spectra of (2*Z*,3*E*)-*N*-cyclohexyl-2,3-bis(cyclohexylimino)-6-methoxy-2,3-dihydrooxazolo[3,2-*a*]indole-9-carboxamide (3j). Purification by column chromatography (EtOAc : hexane v/v 1 : 19) afforded **3j**: yellow solid, yield = 53% (70 mg, 0.140 mmol), ^{1}H NMR (400 MHz, $CDCl_3$): δ 8.00 (d, J = 8.0 Hz, 1H), 7.45 (d, J = 2.4 Hz, 1H), 6.88 (dd, J = 8.8 Hz, 2.4 Hz), 4.77–4.71 (m, 1H), 4.08–3.95 (m, 1H), 3.85 (s, 3H), 2.00–1.24 (m, 30H) ppm. $^{13}C\{^1H\}$ NMR (100 MHz, $CDCl_3$): δ 170.8, 161.9, 156.9, 148.2, 139.5, 134.5, 128.0, 122.3, 122.2, 111.7, 98.3, 87.6, 57.3, 56.4, 55.8, 47.3, 34.0, 33.2, 29.8, 25.9, 25.8, 25.7, 24.5, 24.4, 23.8, 23.1 ppm. HRMS (ESI-TOF) *m*/*z*: $[M + H]^+$ calcd for $C_{30}H_{40}N_4O_3$ 505.3179; found 505.3177.

^{1}H NMR (400 MHz, $CDCl_3$) and $^{13}C\{^1H\}$ NMR (100 MHz, $CDCl_3$) spectra of (2*Z*,3*E*)-*N*-(*tert*-butyl)-2,3-bis(*tert*-butylimino)-7-nitro-2,3-dihydrooxazolo[3,2-*a*]indole-9-carboxamide (3l). Purification by column chromatography (EtOAc : hexane v/v 1 : 19) afforded **3l**: yellow solid, yield = 56% (60.5 mg, 0.137 mmol), ^{1}H NMR (400 MHz, $CDCl_3$): δ 9.15 (d, J = 2.0 Hz, 1H), 8.13 (td, J = 8.8, 2.0 Hz, 1H), 7.96 (d, J = 8.8 Hz, 1H), 5.68 (s, 1H), 1.53 (s, 9H), 1.51 (s, 9H), 1.47 (s, 9H) ppm. $^{13}C\{^1H\}$ NMR (100 MHz, $CDCl_3$): δ 161.2, 149.7, 144.8, 135.0, 132.3, 130.3, 129.2, 119.0, 118.5, 112.4, 88.7, 58.2, 56.6, 51.7, 30.0, 29.34, 29.27, 28.8 ppm. HRMS (ESI-TOF) *m*/*z*: $[M + H]^+$ calcd for $C_{23}H_{32}N_5O_4$ 442.2454; found 442.2463.

^{1}H NMR (700 MHz, $CDCl_3$), $^{13}C\{^1H\}$ NMR (175 MHz, $CDCl_3$) and $^{19}F\{^1H\}$ NMR (376 MHz, $CDCl_3$) spectra of (2*Z*,3*E*)-*N*-(*tert*-butyl)-2,3-bis(*tert*-butylimino)-7-(trifluoromethoxy)-2,3-dihydrooxazolo[3,2-*a*]indole-9-carboxamide (3m). Purification by column chromatography (EtOAc : hexane v/v 1 : 19) afforded **3m**: yellow solid, yield = 37% (36.5 mg, 0.076 mmol), ^{1}H NMR (700 MHz, $CDCl_3$): 8.17 (d, J = 1.4 Hz, 1H), 7.91 (d, J = 9.1 Hz, 1H), 7.11 (dd, J = 8.4, 1.4 Hz, 1H), 5.70 (s, 1H), 1.55 (s, 9H), 1.54 (s, 9H), 1.50 (s, 9H) ppm. $^{13}C\{^1H\}$ NMR (175 MHz, $CDCl_3$): δ 161.8, 149.4, 145.97, 145.96, 135.7, 132.5, 129.9, 125.6, 121.37, 119.91, 116.7, 115.1, 113.1, 88.0, 57.8, 56.0, 51.4, 29.9, 29.3, 29.2 ppm. $^{19}F\{^1H\}$ NMR (376 MHz, $CDCl_3$): −57.86 ppm. HRMS (ESI-TOF) *m*/*z*: $[M + H]^+$ calcd for $C_{24}H_{32}F_3N_4O_3$ 481.2427; found 481.2430.

^{1}H NMR (700 MHz, $CDCl_3$), $^{13}C\{^1H\}$ NMR (175 MHz, $CDCl_3$) and $^{19}F\{^1H\}$ NMR (376 MHz, $CDCl_3$) spectra of (2*Z*,3*E*)-*N*-(*tert*-butyl)-2,3-bis(*tert*-butylimino)-7-fluoro-2,3-dihydrooxazolo[3,2-*a*]-indole-9-carboxamide (3q). Purification by column chromatography (EtOAc : hexane v/v 1 : 19) afforded **3q**: yellow solid, yield = 41% (48 mg, 0.116 mmol), ^{1}H NMR (700 MHz, $CDCl_3$): δ 7.96 (dd, J = 9.8 Hz, 2.8 Hz, 1H), 7.84 (q, J = 4.2 Hz, 1H), 6.95 (td, J = 8.4 Hz, 2.1 Hz, 1H), 5.69 (s, 1H), 1.55 (s, 9H), 1.53 (s, 9H), 1.50 (s, 9H) ppm. $^{13}C\{^1H\}$ NMR (175 MHz, $CDCl_3$): δ 162.0, 160.9, 159.5, 149.4, 135.9, 132.6, 130.2, 130.1, 123.7, 113.3, 113.2, 110.6, 110.5, 108.6, 108.4, 87.9, 57.7, 56.0, 51.4, 29.9, 29.4, 29.3 ppm. $^{19}F\{^1H\}$ NMR (376 MHz, $CDCl_3$): −117.66 ppm. HRMS (ESI-TOF) *m*/*z*: $[M + H]^+$ calcd for $C_{23}H_{32}FN_4O_2$ 415.2509; found 415.2513.

^{1}H NMR (400 MHz, $CDCl_3$) and $^{13}C\{^1H\}$ NMR (100 MHz, $CDCl_3$) spectra of (2*Z*,3*E*)-*N*-(*tert*-butyl)-2,3-bis(*tert*-butylimino)-7-chloro-2,3-dihydrooxazolo[3,2-*a*]indole-9-carboxamide (3r). Purification by column chromatography (EtOAc : hexane v/v 1 : 19) afforded **3r**; yellow solid, yield = 54% (60 mg, 0.140 mmol), ^{1}H NMR (400 MHz, $CDCl_3$): 8.25 (d, J = 2.0 Hz, 1H), 7.78 (d, J = 8.0 Hz, 1H), 7.16 (dd, J = 2.0, 8.0 Hz, 1H), 5.66 (s, 1H), 1.51 (s, 9H), 1.50 (s, 9H), 1.46 (s, 9H) ppm. $^{13}C\{^1H\}$ NMR (100 MHz, $CDCl_3$): δ 161.9, 149.2, 135.9, 132.6, 130.2, 130.0, 125.7, 123.3, 121.9, 113.4, 87.6, 57.8, 56.1, 51.5, 30.0, 29.4, 29.3 ppm. HRMS (ESI-TOF) *m*/*z*: $[M + H]^+$ calcd for $C_{23}H_{32}ClN_4O_2$ 431.2214; found 431.2212.

^{1}H NMR (400 MHz, $CDCl_3$) and $^{13}C\{^1H\}$ NMR (100 MHz, $CDCl_3$) spectra of (2*Z*,3*E*)-7-chloro-*N*-(2,4,4-trimethylpentan-2-yl)-2,3-bis((2,4,4-trimethylpentan-2-yl)imino)-2,3-dihydrooxazolo[3,2-*a*]indole-9-carboxamide (3s). Purification by column chromatography (EtOAc : hexane v/v 1 : 19) afforded **3s**; yellow solid, yield = 46% (71 mg, 0.119 mmol), ^{1}H NMR (400 MHz, $CDCl_3$): δ 8.28 (d, J = 4.0 Hz, 1H), δ 7.83 (d, J = 8.4 Hz, 1H), 7.18 (dd, J = 8.4, 2.0 Hz, 1H), 5.58 (s, 1H), 1.99 (s, 2H), 1.91 (s, 4H), 1.57 (s, 6H), 1.54 (s, 6H), 1.50 (s, 6H), 1.02 (s, 9H), 1.00 (s, 9H), 0.99 (s, 9H) ppm. $^{13}C\{^1H\}$ NMR (100 MHz, $CDCl_3$): δ 161.8, 148.9, 135.5, 131.4, 130.3, 129.9, 125.7, 123.4, 122.0, 113.3, 87.5, 61.6, 60.2, 55.4, 54.3, 54.1, 51.0, 32.14, 32.09, 32.05, 31.9, 31.7, 31.6, 31.0, 30.2, 30.1 ppm. HRMS (ESI-TOF) *m*/*z*: $[M + H]^+$ calcd for $C_{35}H_{56}ClN_4O_2$ 599.4092; found 599.4091.

^{1}H NMR (400 MHz, $CDCl_3$) and $^{13}C\{^1H\}$ NMR (100 MHz, $CDCl_3$) spectra of (2*Z*,3*E*)-7-bromo-*N*-(*tert*-butyl)-2,3-bis(*tert*-butylimino)-2,3-dihydrooxazolo[3,2-*a*]indole-9-carboxamide (3t). Purification by column chromatography (EtOAc : hexane v/v 1 : 19) afforded **3t**: yellow solid, yield = 51% (51 mg, 0.107 mmol), ^{1}H NMR (400 MHz, $CDCl_3$): 8.41 (d, J = 2.0 Hz, 1H), 7.73 (d, J = 8.0 Hz, 1H), 7.30 (dd, J = 2.0, 8.0 Hz, 2H), 5.66 (s, 1H), 1.51 (s, 9H),

1.50 (s, 9H), 1.46 (s, 9H) ppm. $^{13}C\{^1H\}$ NMR (100 MHz, $CDCl_3$): δ 161.9, 149.1, 135.8, 132.6, 130.6, 126.1, 126.0, 124.8, 117.7, 113.8, 87.4, 57.8, 56.1, 51.5, 30.0, 29.4, 29.3 ppm. HRMS (ESI-TOF) *m*/*z*: $[M + H]^+$ calcd for $C_{23}H_{32}BrN_4O_2$ 475.1709; found 475.1709.

^{1}H NMR (400 MHz, $CDCl_3$) and $^{13}C\{^1H\}$ NMR (100 MHz, $CDCl_3$) spectra of (2*Z*,3*E*)-7-bromo-*N*-cyclohexyl-2,3-bis(cyclohexylimino)-2,3-dihydrooxazolo[3,2-*a*]indole-9-carboxamide (3u). Purification by column chromatography (EtOAc : hexane v/v 1 : 19) afforded **3u**: yellow solid, yield = 48% (56 mg, 0.101 mmol), ^{1}H NMR (400 MHz, $CDCl_3$): δ 8.32 (d, J = 2.0 Hz, 1H), 7.71 (d, J = 8.4 Hz, 1H), 7.31 (dd, J = 8.4 Hz, 2.0 Hz, 1H), 5.71 (d, J = 7.6 Hz, 1H), 4.76–4.70 (m, 1H), 4.08–3.96 (m, 1H), 2.00–1.24 (m, 30H) ppm. $^{13}C\{^1H\}$ NMR (100 MHz, $CDCl_3$): δ 161.3, 149.3, 138.7, 134.1, 130.5, 126.1, 125.8, 124.7, 117.7, 114.0, 87.4, 57.6, 56.6, 47.5, 33.9, 33.2, 33.1, 29.8, 25.81, 25.76, 25.7, 24.5, 24.4, 23.8 ppm. HRMS (ESI-TOF) *m*/*z*: $[M + H]^+$ calcd for $C_{29}H_{38}BrN_4O_2$ 553.2178; found 553.2180.

^{1}H NMR (700 MHz, $CDCl_3$) and $^{13}C\{^1H\}$ NMR (175 MHz, $CDCl_3$) spectra of (2*Z*,3*E*)-*N*-(*tert*-butyl)-2,3-bis(*tert*-butylimino)-6-chloro-2,3-dihydrooxazolo[3,2-*a*]indole-9-carboxamide (3v). Purification by column chromatography (EtOAc : hexane v/v 1 : 19) afforded **3v**:; yellow solid, yield = 50% (56 mg, 0.129 mmol), ^{1}H NMR (700 MHz, $CDCl_3$): δ 8.17 (d, J = 8.4 Hz, 1H), 7.90 (d, J = 2.1 Hz, 1H), 7.26 (dd, J = 8.4, 1.4 Hz, 1H), 5.71 (s, 1H), 1.55 (s, 9H), 1.53 (s, 9H), 1.50 (s, 9H) ppm. $^{13}C\{^1H\}$ NMR (175 MHz, $CDCl_3$): δ 161.9, 148.6, 135.9, 132.5, 128.7, 124.50, 122.8, 112.1, 87.8, 57.8, 56.1, 51.4, 29.9, 29.3, 29.2 ppm. HRMS (ESI-TOF) *m*/*z*: $[M + H]^+$ calcd for $C_{23}H_{33}N_4O_2$ 431.2213; found 431.2214.

^{1}H NMR (400 MHz, $CDCl_3$) and $^{13}C\{^1H\}$ NMR (100 MHz, $CDCl_3$) spectra of *N*-(*tert*-butyl)-2-oxoindoline-3-carboxamide (4). Purification by column chromatography (EtOAc : hexane v/v 1 : 9) afforded **4**; off-white solid, yield = 78% (70 mg, 0.301 mmol), ^{1}H NMR (400 MHz, $CDCl_3$): δ 8.25 (s, 1H), 7.69 (d, J = 7.2 Hz, 1H), 7.33 (s, 1H), 7.24 (t, J = 6.8 Hz, 1H), 7.10 (t, J = 7.6 Hz, 1H), 6.87 (d, J = 7.2, 1H), 4.18 (s, 1H), 1.37 (s, 9H) ppm. $^{13}C\{^1H\}$ NMR (100 MHz, $CDCl_3$): δ 175.7, 162.5, 140.5, 128.6, 127.4, 124.4, 123.2, 109.8, 51.7, 51.4, 28.8 ppm. HRMS (ESI-TOF) *m*/*z*: $[M + H]^+$ calcd for $C_{13}H_{16}N_2O_2Na$ 255.1109; found 255.1110.

Conflicts of interest

The authors declare no competing financial interest.

Acknowledgements

We are thankful to the Science and Engineering Research Board (SERB), India (CRG/2021/002077) and Centre of Excellence for Emerging Materials, Thapar Institute of Engineering and Technology, Patiala (TIET/CEEMS/Regular/2022/042) for financial support. Also, we acknowledge the DST-FIST grant (SR/FST/CS-II/2018/69) at the School of Chemistry and Biochemistry, Thapar Institute of Engineering and Technology, Patiala and Single Crystal X-ray Diffraction (SCXRD) facility at the Department of Chemistry, Panjab University, Chandigarh for providing the X-ray crystallography data.

References

1 (*a*) Y. M. Khetmalis, M. Shivani, S. Murugesan and K. V. G. Chandra Sekhar, Oxindole and its derivatives: a review on recent progress in biological activities, *Biomed. Pharmacother.*, 2021, **141**, 111842; (*b*) S. Ravi Suman Rudrangi, V. Kumar Bontha, V. Reddy Manda and S. Bethi, Oxindoles and their pharmaceutical significance-an overview, *Asian J. Res. Chem.*, 2011, **4**, 335–338; (*c*) L. Yin, Q. Hu, J. Emmerich, M. M. C. Lo, E. Metzger, A. Ali and R. W. Hartmann, Novel pyridyl-or isoquinolinyl-substituted indolines and indoles as potent and selective aldosterone synthase inhibitors, *J. Med. Chem.*, 2014, **57**, 5179–5189; (*d*) N. Monakhova, S. Ryabova and V. Makarov, Synthesis and some biological properties of Pyrrolo[1,2-a]indoles, *J. Heterocycl. Chem.*, 2016, **53**, 685–709; (*e*) C. Bunders, J. Cavanagh and C. Melander, Flustramine inspired synthesis and biological evaluation of pyrroloindoline triazole amides as novel inhibitors of bacterial biofilms, *Org. Biomol. Chem.*, 2011, **9**, 5476–5481; (*f*) L. M. Gaste, P. A. Wyman, E. S. Ellis, A. M. Brown and T. J. Young, 5-HT4receptor antagonists: oxazolo, oxazino and oxazepino[3,2-*a*]indole derivatives, *Bioorg. Med. Chem. Lett.*, 1994, **4**, 667–668; (*g*) W. C. Sumpter, THE CHEMISTRY OF ISATIN, *Chem. Rev.*, 1944, **34**, 393–434.

2 (*a*) L. Y. Mei, Y. Wei, X. Y. Tang and M. Shi, Catalyst-Dependent Stereodivergent and Regioselective Synthesis of Indole-Fused Heterocycles through Formal Cycloadditions of Indolyl-Allenes, *J. Am. Chem. Soc.*, 2015, **137**, 8131–8137; (*b*) G. Pan, L. Lu, W. Zhuang and Q. Huang, Synthesis of Indole-Fused Six-, Seven-, or Eight-Membered N, O-Heterocycles via Rhodium-Catalyzed *NH*-Indole-Directed C–H Acetoxylation/Hydrolysis/Annulation, *J. Org. Chem.*, 2021, **86**, 16753–16763; (*c*) X. Fang, S. Gao, Z. Wu, H. Yao and A. Lin, Pd(II)-Catalyzed oxidative dearomatization of indoles: substrate-controlled synthesis of indolines and indolones, *Org. Chem. Front.*, 2017, **4**, 292–296; (*d*) Y. Huang, Y. Yang, H. Song, Y. Liu and Q. Wang, Synthesis of Structurally Diverse 2,3-Fused Indoles via Microwave-Assisted $AgSbF_6$-Catalysed Intramolecular Difunctionalization of *o*-Alkynylanilines, *Sci. Rep.*, 2015, **5**, 13516; (*e*) K. F. Suzdalev, S. V. Den'Kina and V. V. Tkachev, Formation of the same pyrimido[1,2-a]indoles from 1-(oxiran-2-ylmethyl)-1*H*-indole or [1,3]oxazolo[3,2-a]indole derivatives in its reactions with aromatic amines, *Tetrahedron*, 2013, **69**, 8785–8789.

3 M. Zhang, Y. Duan, W. Li, Y. Cheng and C. Zhu, Visible-light-induced aerobic dearomative reaction of indole derivatives: access to heterocycle fused or spirocyclo indolones, *Chem. Commun.*, 2016, **52**, 4761–4763.

4 L. A. Oparina, N. A. Kolyvanov, I. A. Ushakov, A. G. Mal'kina, A. V. Vashchenko and B. A. Trofimov, Metal-and Solvent-free Synthesis of Functionalized Dihydrooxazolo[3,2-*a*]indoles

by One-Pot Tandem Assembly of 3*H*-Indoles and Propargylic Alcohols, *Synthesis*, 2019, 1445–1454.

5 Y. Zhao, X. Niu, H. Yang, J. Yang, Z. Wang and Q. Wang, Substrate-directed divergent synthesis of fused indole polycycles through Rh(II)-catalyzed cascade reactions of bis (diazo) indolin-2-ones, *Chem. Commun.*, 2022, **58**, 8576–8579.

6 (*a*) M. G. Ciulla, S. Zimmermann and K. Kumar, Cascade reaction based synthetic strategies targeting biologically intriguing indole polycycles, *Org. Biomol. Chem.*, 2019, **17**, 413–431; (*b*) X. Ma and W. Zhang, Recent developments in one-pot stepwise synthesis (OPSS) of small molecules, *Iscience*, 2022, **25**, 105005; (*c*) A. Baccalini, G. Faita, G. Zanoni and D. Maiti, Transition Metal Promoted Cascade Heterocycle Synthesis through C−H Functionalization, *Chem. – Eur. J.*, 2020, **26**, 9749–9783; (*d*) I. Alahyen, L. Benhamou, V. Dalla, C. Taillier and S. Comesse, 20 Years of Forging N-Heterocycles from Acrylamides through Domino/Cascade Reactions, *Synthesis*, 2021, 3409–3439; (*e*) R. Connon and P. J. Guiry, Recent advances in the development of one-pot/multistep syntheses of 3,4-annulated indoles, *Tetrahedron Lett.*, 2020, **61**, 151696.

7 (*a*) F. L. Hong and L. W. Ye, Transition metal-catalyzed tandem reactions of ynamides for divergent N-heterocycle synthesis, *Acc. Chem. Res.*, 2020, **53**, 2003–2019; (*b*) A. Cabré, X. Verdaguer and A. Riera, Multi-component syntheses of heterocycles by transition-metal catalysis, *Chem. Rev.*, 2022, **122**, 269–339; (*c*) Y. Xia and J. Wang, Transition-Metal-Catalyzed Cross-Coupling with Ketones or Aldehydes via *N*-Tosylhydrazones, *J. Am. Chem. Soc.*, 2020, **142**, 10592–10605.

8 (*a*) G. Qiu, Q. Wang and J. Zhu, Palladium-Catalyzed Three-Component Reaction of Propargyl Carbonates, Isocyanides, and Alcohols or Water: Switchable Synthesis of Pyrroles and Its Bicyclic Analogues, *Org. Lett.*, 2017, **19**, 270–273; (*b*) Z. Tashrifi, M. Mohammadi Khanaposhtani, F. Gholami, B. Larijani and M. Mahdavi, Rapid Access to Fused Tetracyclic N-Heterocycles via Amino-to-Alkyl 1,5-Palladium Migration Coupled with Intramolecular $C(sp^3)$–$C(sp^2)$ Coupling, *Adv. Synth. Catal.*, 2023, **365**, 926–947; (*c*) J. W. Collet, T. R. Roose, B. Weijers, B. U. W. Maes, E. Ruijter and R. V. A. Orru, Recent advances in palladium-catalyzed isocyanide insertions, *Molecules*, 2020, **25**, 4906; (*d*) F. Zhou, K. Ding and Q. Cai, Palladium-Catalyzed Amidation of *N*-Tosylhydrazones with Isocyanides, *Chem. – Eur. J.*, 2011, **17**, 12268–12271; (*e*) Y. Tian, L. Tian, X. He, C. Li, X. Jia and J. Li, Indium(III) chloride-catalyzed isocyanide insertion reaction to construct complex spirooxindole, *Org. Lett.*, 2015, **17**, 4874–4877.

9 M. Cao, Y. L. Fang, Y. C. Wang, X. J. Xu, Z. W. Xi and S. Tang, $Ce(OTf)_3$-Catalyzed Multicomponent Reaction of Alkynyl Carboxylic Acids, *tert*-Butyl Isocyanide, and Azides for the Assembly of Triazole–Oxazole Derivatives, *ACS Comb. Sci.*, 2020, **22**, 268–273.

10 S. Sisodiya, A. Acharya, M. Nagpure, N. Roy, S. K. Giri, H. R. Yadav, A. R. Choudhury and S. K. Guchhait, A cascade reaction of indolyl-migratory isocyanide insertion, scaffold rearrangement and redox-neutral event with isocyanide as a $C(sp^3)$H–N synthon efficiently constructs indolylisoindolinones, *Chem. Commun.*, 2022, **58**, 11827–11830.

11 S. Lu, C. H. Ding and B. Xu, Triple-Consecutive Isocyanide Insertions with Aldehydes: Synthesis of 4-Cyanooxazoles, *Org. Lett.*, 2023, **25**, 849–854.

12 P. Soam, H. Gaba, D. Mandal and V. Tyagi, A Pd-catalyzed one-pot cascade consisting of C–C/C–O/N–N bond formation to access benzoxazine fused 1,2,3-triazoles, *Org. Biomol. Chem.*, 2021, **19**, 9936–9945.

13 P. Soam, D. Mandal and V. Tyagi, Divergent and Selective Synthesis of 3-Alkylidene Oxindoles Using Pd-Catalyzed Multicomponent Reaction, *J. Org. Chem.*, 2023, **88**, 11023–11035.

14 (*a*) B. Vol, D. H. McDANIEL and H. C. Brown, An extended table of Hammett substitutent constants based on the ionization of substituted benzoic acids, *J. Org. Chem.*, 1958, **23**, 420–427; (*b*) H. M. Yau, R. S. Haines and J. B. Harper, A Robust, ''One-Pot'' Method for Acquiring Kinetic Data for Hammett Plots Used to Demonstrate Transmission of Substituent Effects in Reactions of Aromatic Ethyl Esters, *J. Chem. Educ.*, 2015, **92**, 538–542; (*c*) S. V. Khansole and Y. B. Vibhute, Kinetic of iodination of phenol and substituted phenols by pyridinium iodochloride in methanol, *J. Iran. Chem. Res.*, 2009, **2**, 151–156.

15 X. Zhang, L. W. Chung and Y. D. Wu, New mechanistic insights on the selectivity of transition-metal-catalyzed organic reactions: the role of computational chemistry, *Acc. Chem. Res.*, 2016, **49**, 1302–1310.

16 (*a*) Y. Xia, D. Qiu and J. Wang, Transition-metal-catalyzed cross-couplings through carbene migratory insertion, *Chem. Rev.*, 2017, **117**, 13810–13889; (*b*) Y. Liu, Z. Luo, J. Z. Zhang and F. Xia, DFT calculations on the mechanism of transition-metal-catalyzed reaction of diazo compounds with phenols: O–H insertion versus C–H insertion, *J. Phys. Chem. A*, 2016, **120**, 6485–6492; (*c*) X. Bi, Z. Liu, S. Cao, J. Wu, G. Zanoni and P. Sivaguru, Palladium(II)-catalyzed cross-coupling of diazo compounds and isocyanides to access ketenimines, *ACS Catal.*, 2020, **10**, 12881–12887; (*d*) X. Hui Zhang, Z. Yuan Geng and K. Tai Wang, Theoretical studies on the mechanism of palladium(II)-catalysed *ortho*-carboxylation of acetanilide with CO, *J. Chem. Sci.*, 2014, **126**, 265–272.

17 (*a*) O. Bakulina, A. Inyutina, D. Dar'in and M. Krasavin, Multicomponent reactions involving diazo reagents: a 5 year update, *Molecules*, 2021, **26**, 6563; (*b*) H. Gu, Z. Qiu, Z. Zhang, J. Li and B. Yan, A mechanistic study of $Pd(OAc)_2$-catalyzed intramolecular C–H functionalization reaction involving CO/isonitrile insertion, *Dalton Trans.*, 2015, **44**, 9839–9846.

18 (*a*) F. Chen, C. Zhu and H. Jiang, [3+1+1] Annulation Reaction of Benzo-1,2-Quinones, Aldehydes and Hydroxylamine Hydrochloride: Access to Benzoxazoles with Inorganic Nitrogen Source, *Adv. Synth. Catal.*, 2021, **363**, 2124–2132; (*b*) W. Q. Zhu, Y. C. Fang, W. Y. Han, F. Li, M. G. Yang and Y. Z. Chen, Palladium-catalyzed [2+2+1] annulation: access to chromone-fused cyclopentanones with cyclopropenone as the CO source, *Org. Chem. Front.*, 2021, **8**, 3082–3090.

